Decentralized Voltage Control to Minimize Distribution Power Loss of Microgrids

Changsun Ahn and Huei Peng

***Abstract*—Microgrids that integrate renewable power sources are suitable for rural communities or certain military applications such as forward operation bases. For microgrids that are not connected to the large electric grid, new control strategies must be designed to maintain proper grid voltage and frequency. In addition, microgrids with distributed power sources and load nodes may have frequent reconfiguration in grid architecture. Therefore, the control strategies ideally should be "plug-and-play", i.e., they should not require significant communication or architecture information, and they should work reliably as long as the supply/demand powers are reasonably balanced. Another unique issue of microgrids is the high resistance loss in distribution lines due to the low operating voltage. To reduce power losses, appropriate voltage control at distributed nodes is required which again must work in a plug-and-play fashion. In this paper, we propose a decentralized voltage control algorithm that minimizes power losses for microgrids. Its optimality and plug-and-play nature are demonstrated through comprehensive simulations.**

***Index Terms*—Decentralized control, grid efficiency, microgrid, power loss minimization, renewable energy, voltage control.**

I. Introduction

DISTRIBUTED renewable power sources are being deployed at a rapid pace due to their lower environmental impact, reduced carbon emission, and improved energy diversity and security. These power sources sometimes are installed in rural areas away from the main electric grid, forming microgrids [1]–[4]. They can be used to support small communities, colleges, hospitals, or other buildings that need a reliable and non-interruptible power supply. For military applications, the microgrid concept is especially appealing because military missions require reliable and secure power supply. Reducing the need for fuel delivery is beneficial from both the financial and logistic viewpoints. The U.S. Army found that 50% of the casualties during non-combat missions in Iraq and Afghanistan are related to fuel delivery [5], [6]. Electricity generators account for 22% of fossil fuel consumption in the contingency period [7]. In other words, reducing logistic needs due to delivery of liquid fuels may help to reduce non-combat casualties. The electricity grid for a forward operating base is frequently an islanded microgrid. In these microgrids, electrified vehicles can serve as energy storage systems and provide vehicle-to-grid (V2G) functions using the on-board generators [8]–[10]. The vehicles can also move and be connected to the microgrids at different locations. This reconfigurable characteristic makes the control of military microgrids more challenging but in the meantime is also an opportunity. Electrified military vehicles consume less fuel during driving, which further cuts down the logistic burden.

Frequent changes of configuration and relocations of small tactical military bases require the microgrid to be plug-and-play. To meet the requirement, the power sources should provide additional grid services, including frequency regulation and voltage regulation. Islanded microgrids have little or no inertia components. In such cases, regulating ac frequency is more challenging. A number of control strategies for frequency regulation have been studied [11]–[14] for microgrids. Another attribute of microgrids is their more resistive lines than high voltage network. This results in a more resistive loss rate than traditional transmission network. Therefore, power loss in the microgrid is higher in percentage and voltage or reactive power allocation over the microgrid network should be considered.

For transmission network in the traditional grids, voltage or reactive power allocation is usually determined through optimization with prior knowledge of the grid structure and the operating conditions [15]–[18]. The optimal reactive power flow and the optimal voltage profile, as a result, can be achieved by adjusting capacitors, tab changing transformers, and synchronous compensators. However, for microgrids, especially military microgrids, these approaches are not appropriate due to two reasons. First, it is desirable to have fewer conventional components, such as capacitors, transformers, and synchronous compensators—deploying those devices at the node level are inconvenient and expensive. Secondly, military microgrids must be scalable and re-configurable, and they have frequent "power source failures" (plug-off of vehicles, intermittent renewable power sources). In other words, centralized concepts using full knowledge of the grid structure are not practical. A decentralized control algorithm based on non-conventional reactive power suppliers is desired.

Control strategies to provide reactive power service to a microgrid without using conventional reactive components have been studied [19]–[21]. Research in [22], [23] showed that inverters can supply active and reactive power to a grid with a wide range of power factor even with uncontrollable power sources, such as solar panels. To realize real-time decentralized control strategies, Tanaka designed a decentralized control strategy extracted from off-line optimization results [24], but this control design requires prior knowledge of the grid structure and extensive computations are needed if the grid structure changes. Cagnano [25] suggested an online optimal reactive power control strategy for microgrids, however, it has a centralized architecture.

Manuscript received December 05, 2011; revised May 06, 2012, August 28, 2012, January 01, 2013; accepted February 14, 2013. Date of publication April 12, 2013; date of current version August 21, 2013. This work was supported by the Automotive Research Center (ARC), a U.S. Army center of excellence in modeling and simulation of ground vehicles. Paper no. TSG-00667-2011.

C. Ahn was with the Department of Mechanical Engineering, University of Michigan, Ann Arbor, MI 48105 USA. He is now with the Korea Institute of Machinery and Materials, Daejeon 305-343, Korea (e-mail: sunahn@kimm.re.kr).

H. Peng is with the Department of Mechanical Engineering, University of Michigan, Ann Arbor, MI 48109 USA (e-mail: hpeng@umich.edu).

Color versions of one or more of the figures in this paper are available online at http://ieeexplore.ieee.org.

Digital Object Identifier 10.1109/TSG.2013.2248174

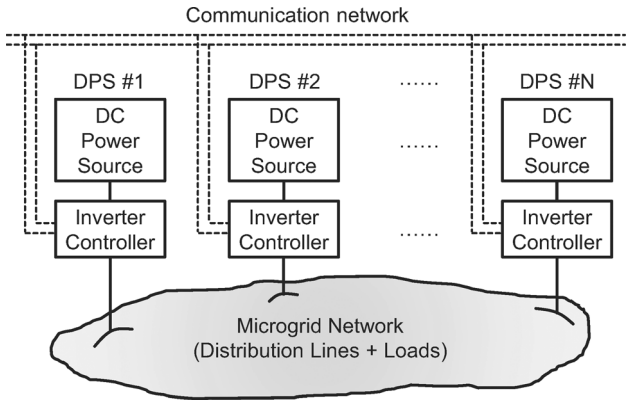

Fig. 1. Example conceptual military microgrid considered in this study for a forward operating base (FOB). The power sources consist of a solar panel and electrified vehicles.

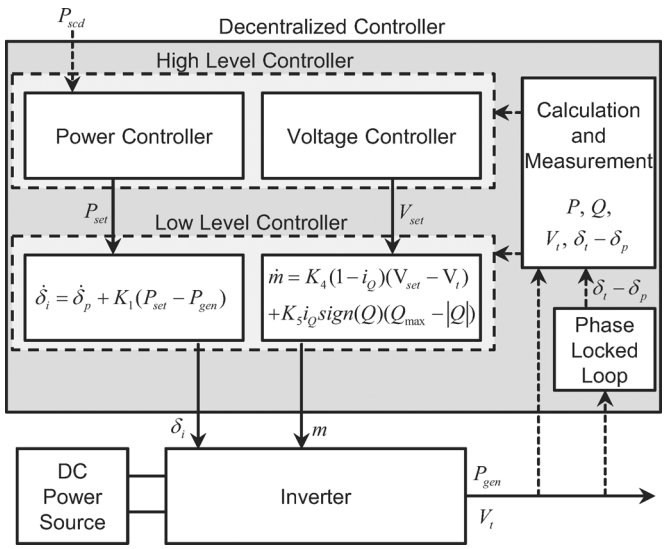

Fig. 2. The structure of the decentralized controller. The High Level Power Controller is described in Section II.C and the High Level Voltage Controller is in Section II-D.

The main contribution of this paper is the development of a model-free, decentralized voltage control algorithm which minimizes power loss of an islanded microgrid through a cost minimization concept. The concept is found to work well even when the configuration of the microgrid changes. The proposed concept consists of two-levels. A low level controller, which is designed based on the inverter and phase-locked loop (PLL) system, regulates the power output and the terminal voltage. The high level controller is designed using a cost function on distribution power loss. We design the high level controller to work in a decentralized way requiring very limited communications.

The remainder of this paper is organized as follows: Section II discusses the controller structure and the decentralized control design, especially the derivation of the high level voltage controller; in Section III, simulation results with plug-and-play performances are presented and discussed; and, finally, conclusions are given in Section IV.

II. Decentralized Controller Design

The structure of the microgrid is shown in Fig. 1, where a communication network may exist (we are analyzing both with and without communication cases). All the distributed

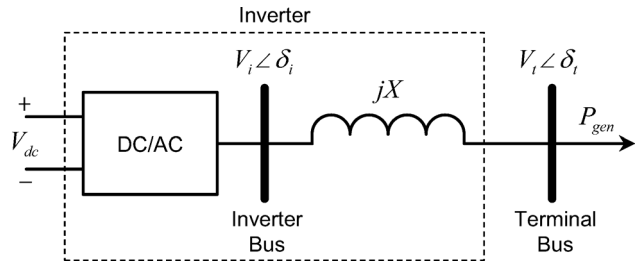

Fig. 3. Inverter model.

power sources are assumed to produce dc, and they can be solar panels, batteries, or wind turbines and internal combustion engine-based generators (such as diesel engine generator or micro turbine generators) that have their power converted to dc (which is a common practice). In this section, we describe the inverter model and controllers, both of which are located in the "Inverter Controller" block in Fig. 1. The details of the controller is shown in Fig. 2 where the controller consists of a high level controller, a low level controller, a phase-locked loop (PLL), and a calculation and measurement block.

A. Inverter Model

The inverter model is shown in Fig. 3, which consists of a dc to ac inverter and a grid interface. The voltage at the inverter bus is synthesized to an ac voltage wave form and the voltage at the terminal bus is common with the grid side. The primary goals of the inverters are to regulate the terminal bus voltage magnitude V_t and the active power delivered to the grid $P_{\rm gen}$. This is achieved by controlling the modulation index m of the inverter, which controls the inverter voltage magnitude V_i through the relationship

$$V_i = mV_{\rm dc}, \tag{1}$$

and the inverter firing angle, which determines the phase angle δ_i. The active power delivered to the grid is then

$$P_{\rm gen} = \frac{V_i V_t}{X}\sin(\delta_i - \delta_t). \tag{2}$$

The two control variables, m and δ_i, are controlled by the low level controller shown in Fig. 2.

B. Low Level Controller

The low-level control is assumed to use a PLL to ensure synchronization to the ac-side voltage. Specifically, the inverter control strategy proposed by Hiskens and Fleming [26] is utilized:

$$\begin{aligned} \theta &= \delta_i - \delta_p, \quad \dot\theta = K_1(P_{\rm set} - P_{\rm gen}),\\ \dot\omega_p &= K_2(\delta_t - \delta_p) + K_3\dot\theta, \quad \dot\delta_p = \omega_p, \end{aligned} \tag{3}$$

where $P_{\rm set}$ is the desired active power assigned by the high level controller, $P_{\rm gen}$ is the active power output, and δ_p is a phase angle observed by the PLL. The design parameters, $K_1 \sim K_3$, are selected to attenuate transient signals (using K_3) and guarantee the tracking performance (using K_1 and K_2).

The terminal voltage V_t is regulated by controlling V_i, which can be achieved by the modulation index control:

$$\dot m = K_4(1 - i_Q)(V_{\rm set} - V_t) + K_5 i_Q\,\mathrm{sign}(Q)(Q_{\max} - |Q|), \tag{4}$$

where V_{set} is the desired voltage given by the high level controller, $Q_{\max}$ and i_Q are determined by

$$Q_{\max} = \sqrt{S_{\max}^2 - P^2}, \quad i_Q = \begin{cases} 1, & \text{if } |Q| \geq Q_{\max} \\ 0, & \text{if } |Q| < Q_{\max} \end{cases}, \tag{5}$$

where $S_{\max}$ is the apparent power limit of the power source, The first term on the right side of (4) is activated only when the magnitude of the current reactive power is smaller than the limitation, and the voltage is being controlled (voltage control mode). Once the reactive power exceeds $Q_{\max}$, then the second term is activated and reactive power is controlled (reactive power control mode). This discrete control structure enables voltage control while keeping the reactive power within the limit. $K_1 \sim K_5$ are adjustable control gains.

C. High Level Power Controller

The active power output should match with the load, which can be done by regulating the grid frequency. For load matching, we assume a PI control is used to regulate the frequency, as follows:

$$P_{\text{set}} = K_P \Delta\omega + K_I \int \Delta\omega \, dt, \tag{6}$$

where K_P and K_I are proportional and integral gains, and $\Delta\omega$ is the frequency error. The frequency error is calculated by subtracting the frequency measured at PLL from the nominal frequency. The nominal frequency is a predefined value as reference, such as 60 Hz.

D. High Level Voltage Controller

When the supply and demand powers are balanced and the frequency is well regulated, the distribution loss is simply a function of voltages at the generator buses. We define the cost function to be minimized in such a case as:

$$P_{\text{Loss}}(\mathbf{V}) = P_G(\mathbf{V}) - P_L = \sum_{i=1}^{N} P_{Gi}(\mathbf{V}) - \sum_{j=1}^{M} P_{Lj}, \tag{7}$$

where P_{Loss} is the total power loss in the grid network, $\mathbf{V} = [V_1, V_2, \ldots, V_N]^T$, P_G is the total power generation, P_{Gi} is the power supplied from the generator bus $\#i$ to the grid, and P_{Lj} is the power consumed at load bus $\#j$ which are assumed to be constant. N is the number of generator buses and M is the number of load buses. The cost function is minimized by controlling the voltages at the generator buses, $V_1, V_2, \ldots, V_N$. The condition for monotonically decreasing $P_{\text{Loss}}(\mathbf{V})$ is:

$$\begin{aligned} \frac{\partial P_{\text{Loss}}(\mathbf{V})}{\partial t} &= \frac{\partial P_G(\mathbf{V})}{\partial t} - \frac{\partial P_L}{\partial t} \\ &= \frac{\partial P_G(\mathbf{V})}{\partial t} = \left(\frac{\partial P_G(\mathbf{V})}{\partial \mathbf{V}}\right)^T \frac{\partial \mathbf{V}}{\partial t} \leq 0, \end{aligned} \tag{8}$$

where P_L is assumed to be constant (or slow varying). To ensure that (8) holds, two algorithms are proposed: a decentralized algorithm with communication and a decentralized algorithm without communication.

In the cases when communication is available, if the control law is chosen to be:

$$\frac{\partial \mathbf{V}}{\partial t} = -k \frac{\partial P_G(\mathbf{V})}{\partial \mathbf{V}}, \tag{9}$$

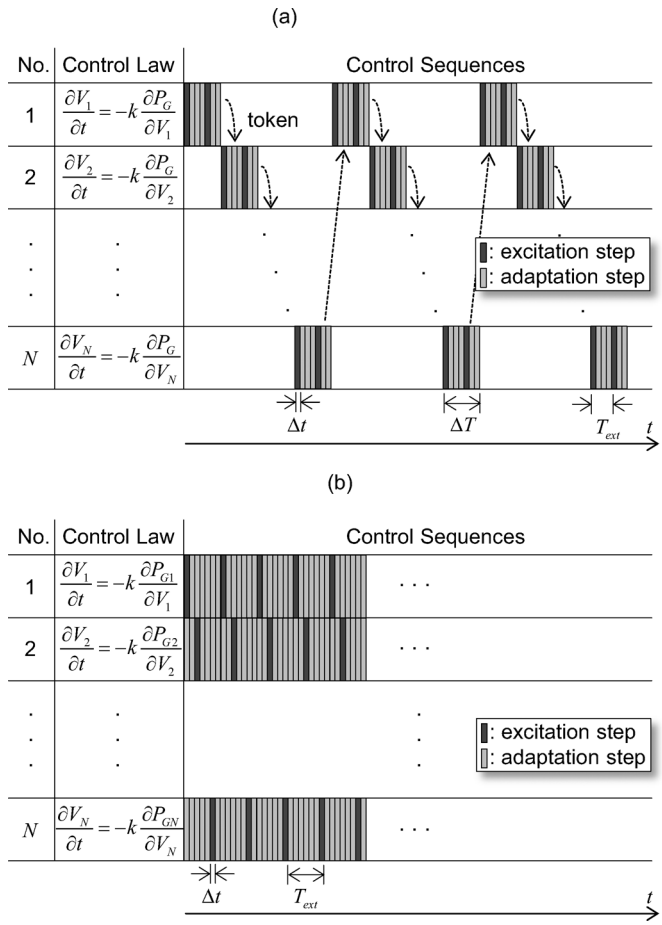

Fig. 4. Conceptual control sequences of the voltage control algorithms. The variables are defined as follows: Δt is a time step; ΔT is a control time span; T_{ext} is a excitation period; and, ΔV_{ext} is a magnitude of voltage excitation. Control actions of each step are described Figs. 5 and 6. (a) Control sequences when a communication network exists. (b) Control sequences when a communication network does not exist.

where k is a positive real number, then (9) always holds because

$$\begin{aligned} \frac{\partial P_G(\mathbf{V})}{\partial t} &= \left(\frac{\partial P_G(\mathbf{V})}{\partial \mathbf{V}}\right)^T \frac{\partial \mathbf{V}}{\partial t} \\ &= -k \left(\frac{\partial P_G(\mathbf{V})}{\partial \mathbf{V}}\right)^T \frac{\partial P_G(\mathbf{V})}{\partial \mathbf{V}} \\ &= -k \left\| \frac{\partial P_G(\mathbf{V})}{\partial \mathbf{V}} \right\|^2 \leq 0. \end{aligned} \tag{10}$$

The control law, (9), can be implemented by measuring the sensitivity of total power generation over voltage variations. It requires the measurement of total generating power and a control authority on all the generator bus voltages, which is a centralized control concept if implemented directly. The requirement for central control authority can be removed by using sequential executions and of the voltage control. To implement the sequential executions, two pieces of information are required: the amount of active power generation of all generators, and a token. Each generator broadcasts its power generation. The token allows only one node to adjust its voltage at any time while all other power sources keep their bus voltage constant, as shown in Figs. 4(a) and 5.

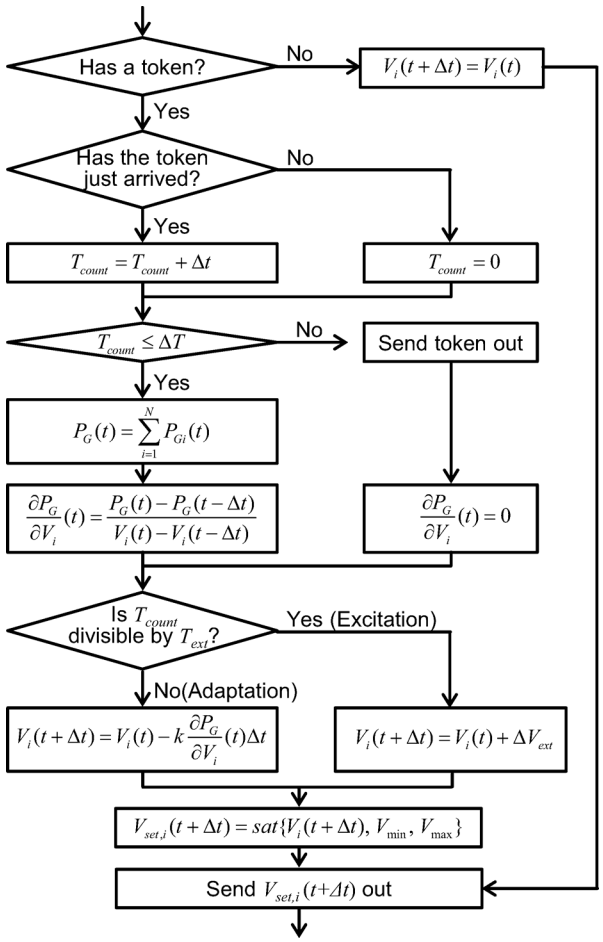

Fig. 5. Control flow in case of that communication is available. The variables are defined as follows: $T_{\rm count}$ is a time counter; Δt is a time step; ΔT is a control time span; T_{ext} is a excitation period; ΔV_{ext} is a magnitude of voltage excitation; $V_{\min}$ is a voltage lower limit; and, $V_{\max}$ is a voltage upper limit.

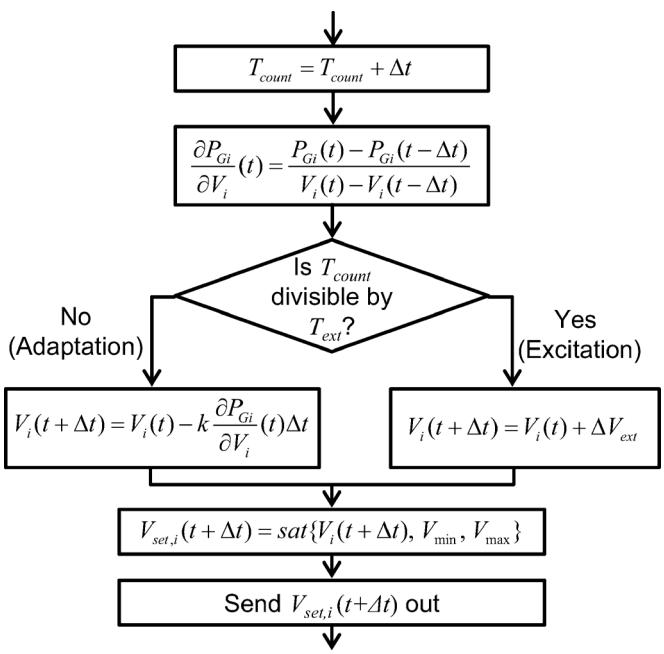

Fig. 6. Flow chart of the voltage control algorithm when communication is not available.

In case that no communication is available, each generator node has access only to local information. The condition for monotonically decreasing $P_{\rm Loss}$ is:

$$\frac{\partial P_G(\mathbf{V})}{\partial t}=\frac{\partial\sum_{i=1}^{N}P_{Gi}(\mathbf{V})}{\partial t}=\sum_{i=1}^{N}\frac{\partial P_{Gi}(\mathbf{V})}{\partial t}$$
$$=\sum_{i=1}^{N}\left(\frac{\partial P_{Gi}(\mathbf{V})}{\partial\mathbf{V}}\right)^T\frac{\partial\mathbf{V}}{\partial t}\le 0. \tag{11}$$

Due to the lack of global information and authority, monotonic decrease of the cost function can be achieved only by using local information. A candidate control law is

$$\frac{\partial V_i}{\partial t}=-k\frac{\partial P_{Gi}(\mathbf{V})}{\partial V_i}, \tag{12}$$

where k is positive real. Plugging (12) into (11):

$$\frac{\partial P_G(\mathbf{V})}{\partial t}=\sum_{i=1}^{N}\left(\frac{\partial P_{Gi}(\mathbf{V})}{\partial\mathbf{V}}\right)^T\frac{\partial\mathbf{V}}{\partial t}$$
$$=\sum_{i=1}^{N}\left[\frac{\partial P_{Gi}}{\partial V_1}\ \cdots\ \frac{\partial P_{Gi}}{\partial V_N}\right]\left[-k\frac{\partial P_{G1}}{\partial V_1}\ \cdots-k\frac{\partial P_{GN}}{\partial V_N}\right]^T$$
$$=-k\sum_{i=1}^{N}\frac{\partial P_{Gi}}{\partial V_i}\left(\frac{\partial P_{Gi}}{\partial V_1}+\cdots+\frac{\partial P_{Gi}}{\partial V_N}\right). \tag{13}$$

The sign of (13) is uncertain. However, if all the distributed controllers use the same control strategy, such as a PI control for frequency droop control, then

$$\Delta P_{G1}=\Delta P_{G2}=\cdots=\Delta P_{GN}=\frac{1}{N}\Delta P_G. \tag{14}$$

Equation (14) then can be rewritten as:

$$\frac{\partial P_G}{\partial t}=-k\sum_{i=1}^{N}\frac{\partial P_{Gi}}{\partial V_i}\left(\frac{\partial P_{Gi}}{\partial V_1}+\cdots+\frac{\partial P_{Gi}}{\partial V_N}\right)$$
$$=-k\sum_{i=1}^{N}\frac{1}{N}\frac{\partial P_G}{\partial V_i}\left(\frac{1}{N}\frac{\partial P_G}{\partial V_1}+\cdots+\frac{1}{N}\frac{\partial P_G}{\partial V_N}\right)$$
$$=-\frac{k}{N^2}\left(\frac{\partial P_G}{\partial V_1}+\cdots+\frac{\partial P_G}{\partial V_N}\right)^2\le 0, \tag{15}$$

In other words, the control law (12) can reduce the power losses using only local information when (14) is satisfied. The control law is implemented as the flowchart shown in Figs. 4(b) and 6.

The controller is implemented in each power source with limited communication. Furthermore, in the controller design, we assume small distribution network and small voltage drops over the network. Therefore, we do not consider voltage level monitoring at load buses. If the load voltage constraints are necessary, we need voltage sensors at the load buses and a higher level of control such as adjusting $V_{\min}$ and $V_{\max}$. However, this requires a centralized control action and, thus, we focus on only the proposed method without voltage sensors at the load buses in this

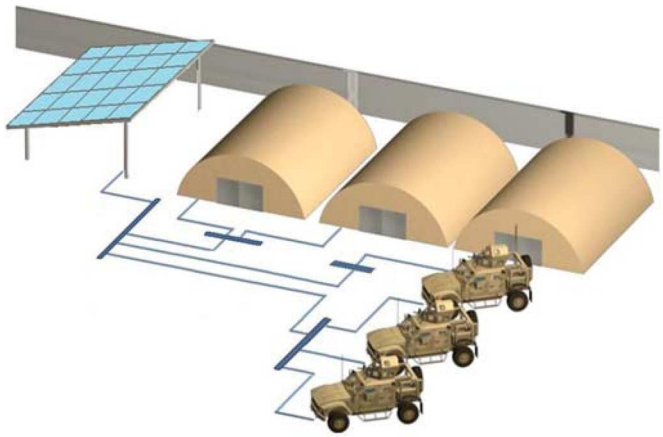

Fig. 7. An imagined military microgrid and grid model. The power sources consist of an array of solar panels and a fleet of electrified vehicles.

paper for the decentralized capability. This may limit the applicability of this method to large grids.

III. Simulation Study

The proposed decentralized algorithms were tested on a simulated grid model of a military forward operating base. The base is assumed to have 50 soldiers and is supported by distributed solar panels and electrified vehicles, as shown in Fig. 7. In the first example, the electric grid consists of two supply buses and two demand buses. In the simulation, we modeled the solar panel and vehicles as voltage sources and assumed that the voltage variations of the dc power sources are well regulated by their own management system and the vehicle batteries can be charged by combustion engine as required. Because the main interest in this research is power loss minimization along long time horizons rather than voltage stability in a short time scale, we modeled the power sources as constant voltage sources. The grid model and controllers were implemented and simulated in Matlab environment.

A. Decentralized Control Algorithm With Communication

The grid model is shown in Fig. 8(a), where 'PV' denotes photovoltaic solar panels. The power from the vehicles was controlled to regulate the frequency. Initially, the solar panels were producing 79.5 kW and vehicles were charging at 10.6 kW. The voltage variations at the generator nodes are limited at $\pm 5\%$ from the nominal value. The grid parameters and initial conditions are listed in the Appendix.

Under the proposed control algorithm, V_1 and V_2 approach 1.05 pu and 1.035 pu, as shown in Fig. 8(b). The overall distribution loss was found to converge to the minimum power loss, the value of which was computed through exhaustive numerical search. Because the power flows from Bus 1 to Bus 2 and the reactive power flow was quite small, V_1 turned out to be higher than V_2. The power loss first reduces quickly with the two bus voltages drift away from each other, then reduces slowly as the two voltage increase together. The total loss is reduced from 7.5% to 5.5%, i.e., by properly setting the voltages of the nodes, the loss is reduced by about 25%. Fig. 8(c) shows the case when the grid load varies in a way similar to what are typically seen during a day. From 0 seconds to 400 seconds, V_1 is higher than

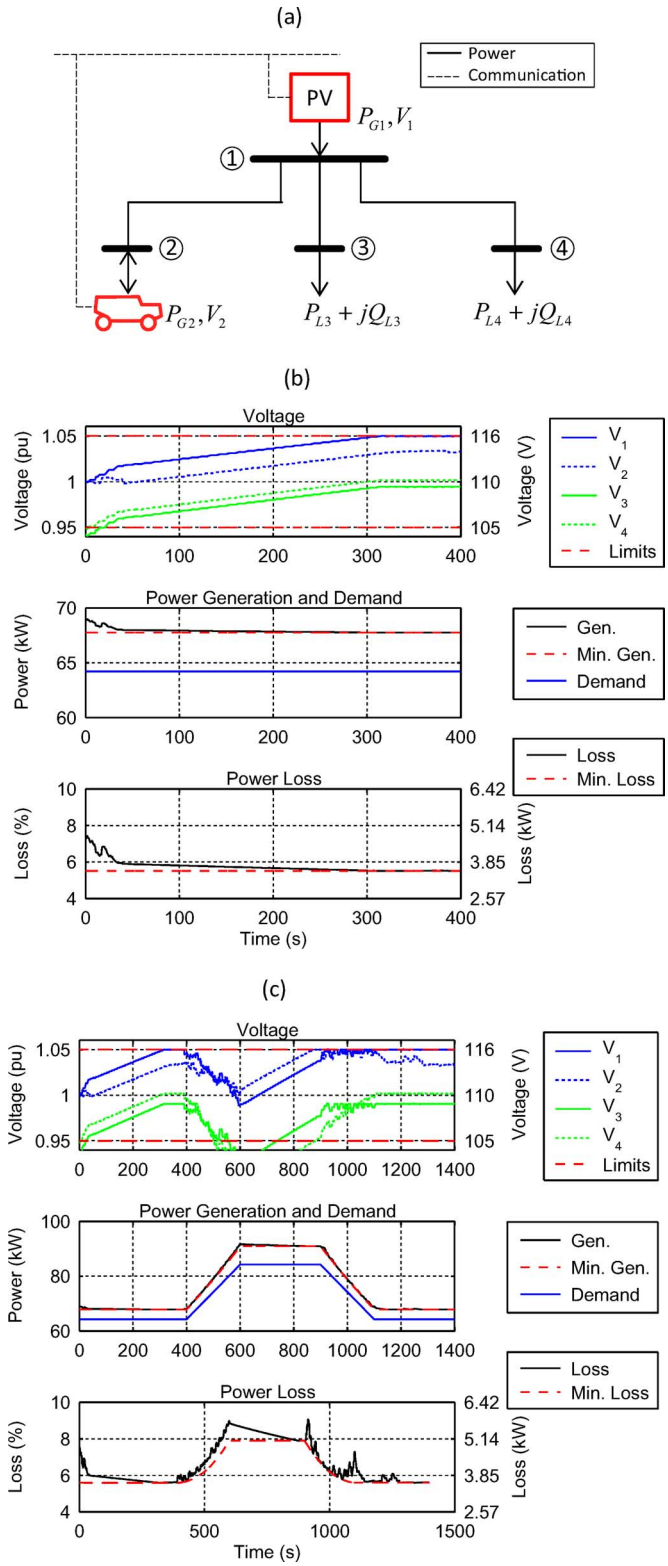

Fig. 8. An imagined military microgrid and grid model. The power sources consist of an array of solar panels and a fleet of electrified vehicles. (a) Grid model. (b) Constant demand case. (c) Varying demand case.

V_2 because power flows from Bus 1 to Bus 2. However, at 600 seconds, demand exceeds the supply level from the solar panels, thus the electrified vehicles provided power back to the grid. In this case, power flows from Bus 2 to Bus 1, and V_2 is higher than V_1. Between 600–900 seconds, the bus voltages increase

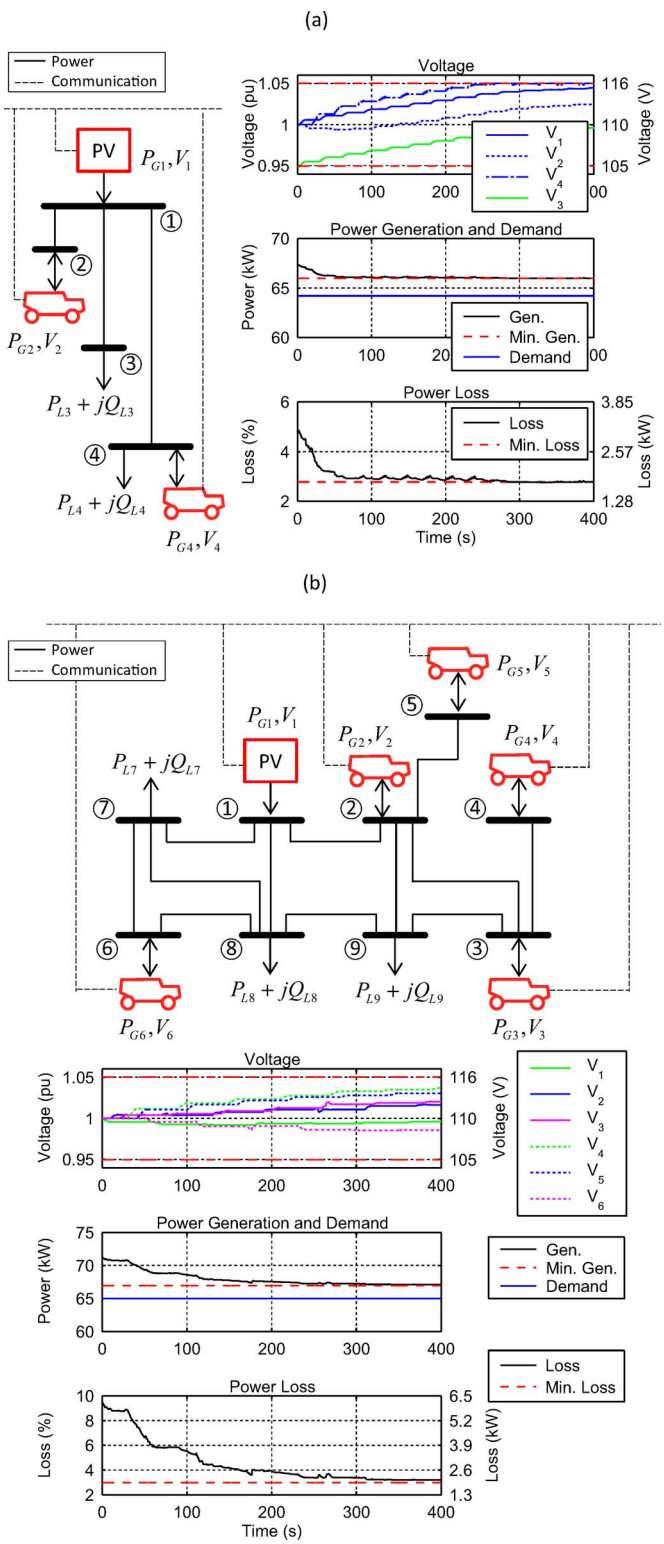

Fig. 9. Scalability of the voltage control algorithm: (a) when a vehicle plugs in Bus 4; (b) when five vehicles plug on a grid with nine buses. The loss (%) is defined as % of total demand. (a) Five buses and three power sources. (b) Nine buses and six power sources.

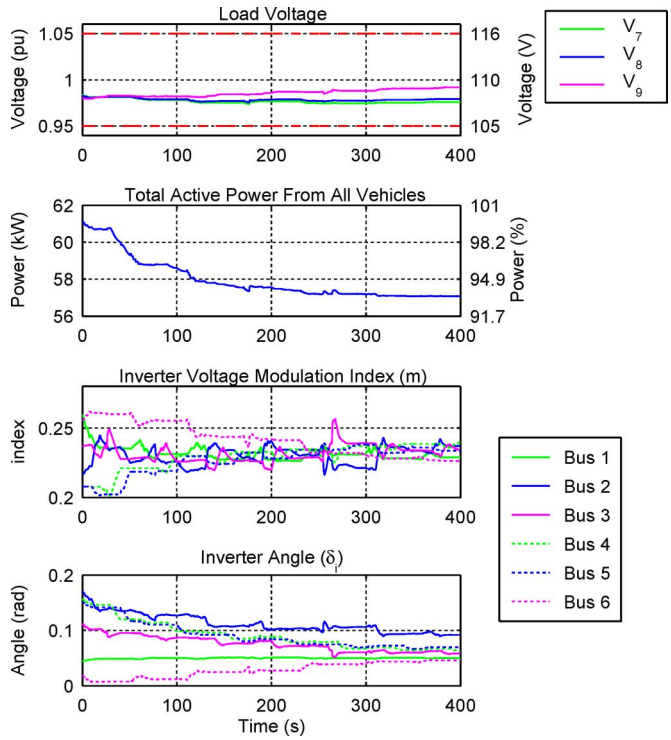

Fig. 10. Load voltage, total power from all vehicles, and control variables for the case of nice buses [Fig. 9(b)]. The total power from the all vehicles reduced by 6.5%.

together to reduce losses. The results show that the decentralized controller works well even when the load changes slowly.

The scalability and flexibility of the control algorithm is further tested under different grid configurations. Distributed power sources, especially electrified vehicles, can be relocated to other buses due to mission requirement. Figs. 9 and 10 show the performance of the voltage controller under changing grid structures. The grid parameters are the same as the previous simulation. For Fig. 9(a), a fleet of vehicles was connected to Bus 4 and supplied power to the grid running on-board generators. Similar to the previous cases, the power loss reduces quickly at the beginning and then slowly approached the minimum value. In this case, the power loss was reduced to 2.8% because the newly connected vehicles collocate with a significant grid loads and thus less grid power flows through the distribution lines. In the case of Fig. 9(b) the grid has nine buses. The proposed algorithm works well in all these cases without using any grid information. Fig. 10 shows changes of control variables and reduction of power from vehicles, where we see 6.5% of power reduction from vehicles. As the number of grids and control variables increase, the convergence is slower because of the higher grid complexity. However, it is also observed that the power loss reduction is greater. The two simulation cases shown in Fig. 9 indicate that the algorithm can adapt to significant grid structure changes and work in a plug-and-play fashion quite reliably.

B. Verification of the Decentralized Control Algorithm Without Communication

The grid used to verify the decentralized control algorithm without communication is shown in Fig. 11. To meet the condition (14), the PV is replaced with a vehicle and all vehicles use the same power controller. Even though there is no communications, all the power output variations are the same because the power output variations are governed by the same controllers using the common signal, the ac frequency. In case when some

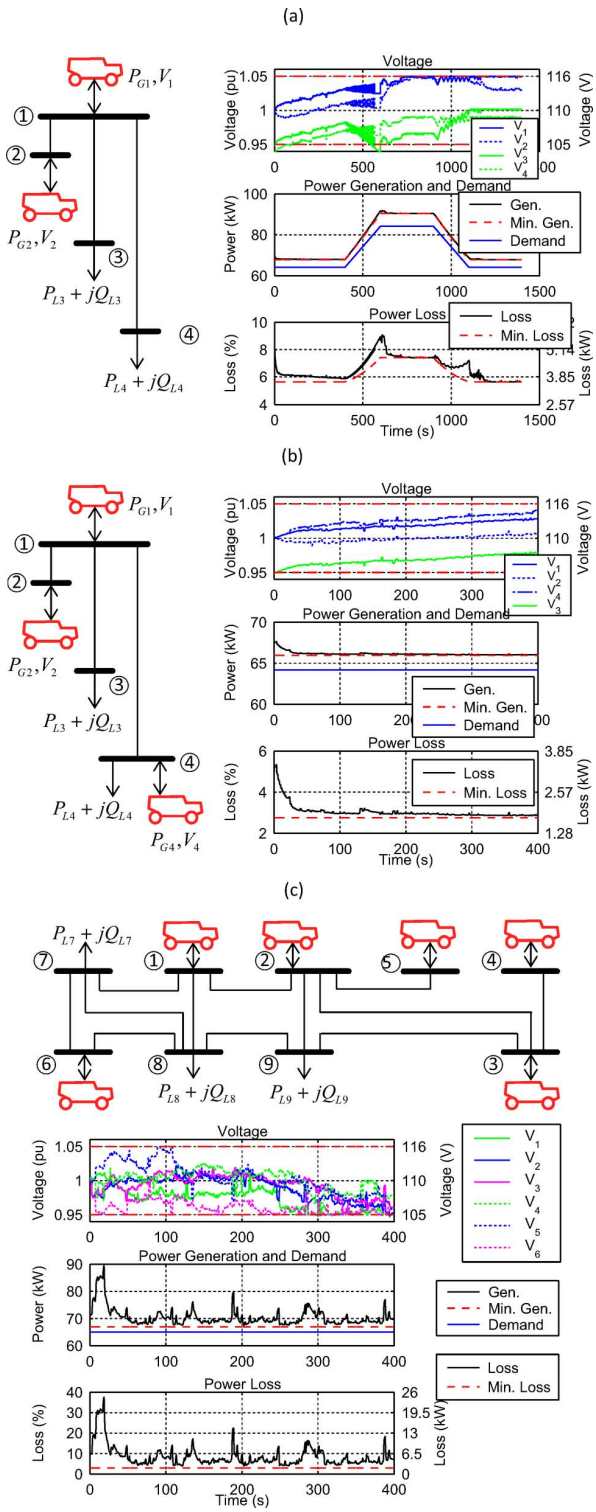

Fig. 11. Performance of voltage control algorithm without communication: (a) under varying demand; (b) when a vehicle plugs in Bus 4; and (c) when six vehicles plug on a grid with nine buses. (a) Four buses and two power sources with time varying demand. (b) Four buses and three power sources. (c) Nine buses and six power sources.

of the distributed power sources and their controllers are different, such one PV with several vehicles, (15) will not hold. The grid parameters and conditions are again those shown in Tables I and II. Verification of the algorithm was performed for both constant demand case and varying demand case. In the constant demand case, shown in Fig. 11(b), the power loss reduction was found to be comparable to the case with communications. However, when the demand power is varying [e.g., Fig. 11(a)], convergence is slower. Furthermore, when the grid structure changed, the algorithm without communication did not quite reach the minimum loss conditions [Fig. 11(b)] and had fluctuating performance [Fig. 11(c)], which show the limitation of communication independent control strategy. Based on these results, we believe the proposed decentralized control WITH communication is a more reliable algorithm to use if it can be made available. The existence of an information network improves the flexibility in power control design and ensures minimum distribution loss is achieved.

IV. Conclusion

Microgrids can have significant distribution losses because of their lower voltage levels. They require a voltage control algorithm that works in a plug-and-play way. In this paper, we proposed two decentralized voltage control algorithms that are derived from a cost function that minimizes power losses over the grid network. Computer based simulation showed that the algorithm can work reliably without knowledge of the operating conditions and grid structure. When communications are not available, the control algorithm still works well in many cases but the performance deteriorates noticeably compared with the case with communication.

Appendix

TABLE I
Grid Parameters

Symbol	Value	Unit	Description
R_L	0.016	pu	Distribution Line resistance
X_L	0.008	pu	Distribution Line reactance

All distribution lines are assumed to be identical. The base voltage is 110V, the base power is 10kW.

TABLE II
Initial Conditions for All the Simulations

Symbol	Value	Unit	Description
P_{L3}	3	pu	Active power demand at Bus 3
P_{L4}	3.42	pu	Active power demand at Bus 4
Q_{L3}, Q_{L4}	0	pu	Reactive power demand at Bus 3 and 4
P_{G1}	7.95	pu	Power from PV, constant
P_{G2}	-1.34	pu	Power from vehicles
V_1, V_2	1	pu	Voltages of Buses 1 and 2

The base voltage is 110V, the base power is 10kW. P_{G2}, V_1, and V_2 vary as the controllers are engaged.

TABLE III
Control Parameter Values

Parameters	Value	Parameters	Value
K_1	20	Δt	0.1 (sec)
K_2	20	ΔT	0.5 (sec)
K_3	10	T_{ext}	0.5 (sec)
K_4	10	ΔV_{ext}	0.0005 (pu)
K_5	10		

REFERENCES

[1] R. Lasseter, A. Akhil, C. Marnay, J. Stephens, J. Dagle, R. Guttromson, A. S. Meliopoulous, R. Yinger, and J. Eto, "Integration of distributed energy resources: The CERTS microgrid concept," U.S. Department of Energy and California Energy Commission, LBNL-50829, 2002.

[2] N. Hatziargyriou, H. Asano, R. Iravani, and C. Marnay, "Microgrids," *IEEE Power Energy Mag.*, vol. 5, pp. 78–94, Jul./Aug. 2007.

[3] R. H. Lasseter and P. Paigi, "Microgrid: A conceptual solution," in *Proc. IEEE Power Electron. Specialists Conf.*, Aachen, Germany, 2004, pp. 4285–4290.

[4] J. M. Guerrero, "Microgrids: Integration of distributed energy resources into the smart-grid," in *Proc. IEEE Int. Symp. Ind. Electron.*, Bari, Italy, 2010, pp. 4281–4414.

[5] D. S. Eady, S. B. Siegel, R. S. Bell, and S. H. Dicke, "Sustain the Mission Project: Casualty factors for fuel and water resupply convoys," Army Environmental Policy Institute, Arlington, VA, USA, Final Tech. Rep. CTC-CR-2009-163, 2009.

[6] G. Baffet, A. Charara, and D. Lechner, "Estimation of vehicle sideslip, tire force and wheel cornering stiffness," *Control Eng. Practice*, vol. 17, pp. 1255–1264, Nov. 2009.

[7] "Army energy security implementation strategy," U.S. Army. Washington, DC, USA, 2009.

[8] W. Kempton and J. Tomic, "Vehicle-to-grid power implementation: From stabilizing the grid to supporting large-scale renewable energy," *J. Power Sources*, vol. 144, pp. 280–294, 2005.

[9] T. Ersal, C. Ahn, I. A. Hiskens, H. Peng, and J. L. Stein, "Impact of controlled plug-in EVs on microgrids: A military microgrid example," in *Proc. IEEE Power Energy Soc. Gen. Meet.*, Detroit, MI, USA, 2011, pp. 1–7.

[10] C. Ahn, C.-T. Li, and H. Peng, "Optimal decentralized charging control algorithm for electrified vehicles connected to smart grid," *J. Power Sources*, vol. 196, pp. 10369–10379, Dec. 2011.

[11] K. De Brabandere, B. Bolsens, J. Van den Keybus, A. Woyte, J. Driesen, R. Belmans, and K. U. Leuven, "A voltage and frequency droop control method for parallel inverters," in *Proc. IEEE Power Electron. Specialists Conf.*, Aachen, Germany, 2004, pp. 2501–2507.

[12] A. Engler and N. Soultanis, "Droop control in LV-grids," in *Proc. Int. Conf. Future Power Syst.*, Amsterdam, The Netherlands, 2005, pp. 1–6.

[13] M. Tokudome, K. Tanaka, T. Senjyu, A. Yona, T. Funabashi, and K. Chul-Hwan, "Frequency and voltage control of small power systems by decentralized controllable loads," in *Proc. Int. Conf. Power Electron. Drive Syst.*, Taipei, Taiwan, 2009, pp. 666–671.

[14] J. M. Guerrero, J. C. Vasquez, J. Matas, L. G. de Vicuna, and M. Castilla, "Hierarchical control of droop-controlled AC and DC microgrids—A general approach toward standardization," *IEEE Trans. Ind. Electron.*, vol. 58, pp. 158–172, Jan. 2011.

[15] A. Kishore and E. F. Hill, "Static optimization of reactive power sources by use of sensitivity parameters," *IEEE Trans. Power App. Syst.*, vol. PAS-90, pp. 1166–1173, 1971.

[16] D. T. W. Sun and R. R. Shoults, "A preventive strategy method for voltage and reactive power dispatch," *IEEE Trans. Power App. Syst.*, vol. PAS-104, pp. 1670–1676, 1985.

[17] S. Granville, "Optimal reactive dispatch through interior point methods," *IEEE Trans. Power Syst.*, vol. 9, pp. 136–146, 1994.

[18] H. Yoshida, K. Kawata, Y. Fukuyama, S. Takayama, and Y. Nakanishi, "A particle swarm optimization for reactive power and voltage control considering voltage security assessment," *IEEE Trans. Power Syst.*, vol. 15, pp. 1232–1239, Nov. 2000.

[19] J. C. Vasquez, R. A. Mastromauro, J. M. Guerrero, and M. Liserre, "Voltage support provided by a droop-controlled multifunctional inverter," *IEEE Trans. Ind. Electron.*, vol. 56, pp. 4510–4519, 2009.

[20] R. A. Mastromauro, M. Liserre, T. Kerekes, and A. Dell'Aquila, "A single-phase voltage-controlled grid-connected photovoltaic system with power quality conditioner functionality," *IEEE Trans. Ind. Electron.*, vol. 56, pp. 4436–4444, 2009.

[21] M. Braun, "Reactive power supply by distributed generators," in *Proc. IEEE Power Energy Soc. Gen. Meet.*, Pittsburgh, PA, USA, 2008, pp. 1–8.

[22] A. Cagnano, F. Torelli, F. Alfonzetti, and E. De Tuglie, "Can PV plants provide a reactive power ancillary service? A treat offered by an on-line controller," *Renewable Energy*, vol. 36, pp. 1047–1052, Mar. 2011.

[23] M. Braun, "Reactive power supplied by PV inverters—Cost-benefit analysis," in *Proc. Eur. Photovoltaic Solar Energy Conf. Exhib.*, Milan, Italy, 2007, pp. 1–7.

[24] K. Tanaka, T. Senjyu, S. Toma, A. Yona, T. Funabashi, and C.-H. Kim, "Decentralized voltage control in distribution systems by controlling reactive power of inverters," in *Proc. IEEE Int. Symp. Ind. Electron.*, Seoul, Korea, 2009, pp. 1385–1390.

[25] A. Cagnano, T. De Tuglie, M. Liserre, and R. A. Mastromauro, "Online optimal reactive power control strategy of PV-inverters," *IEEE Trans. Ind. Electron.*, vol. 58, pp. 4549–4558, Oct. 2011.

[26] I. A. Hiskens and E. M. Fleming, "Control of inverter-connected sources in autonomous microgrids," in *Proc. Amer. Control Conf.*, Seattle, WA, USA, 2008, pp. 586–590.

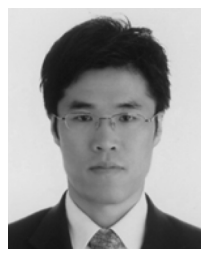

Changsun Ahn received the B.S. and M.S. degrees from Seoul National University, Korea, in 1999 and 2005, respectively, and the Ph.D. degree from the University of Michigan, Ann Arbor, MI, USA, in 2011, all in mechanical engineering.

He is a Senior Researcher in Korea Institute of Machinery and Materials, Daejon, South Korea. His research interests include the fields of automotive control/estimation and energy system control. Recently, he focuses on the energy flow control of smart grids and microgrids especially having plug in electric vehicles.

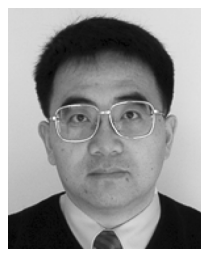

Huei Peng received his Ph.D. from the University of California, Berkeley, Ca, USA, in 1992. He is currently a Professor at the Department of Mechanical Engineering, and the Executive Director of Interdisciplinary and Professional Engineering, at the University of Michigan, Ann Arbor, MI, USA. His research interests include adaptive control and optimal control, with emphasis on their applications to vehicular and transportation systems. His current research focuses include design and control of hybrid electric vehicles and vehicle active safety systems.

Dr. Peng has been an active member of the Society of Automotive Engineers (SAE) and the ASME Dynamic System and Control Division (DSCD). He served as the chair of the ASME DSCD Transportation Panel from 1995 to 1997, and is a member of the Executive Committee of ASME DSCD. He served as an Associate Editor for the IEEE/ASME Transactions on Mechatronics from 1998–2004 and for the ASME Journal of Dynamic Systems, Measurement and Control from 2004–2009. He received the National Science Foundation (NSF) Career award in 1998. He is an ASME Fellow.